

UCLA

UCLA Previously Published Works

Title

Illustrated Neuropathologic Diagnosis of Alzheimers Disease.

Permalink

<https://escholarship.org/uc/item/7946t0v3>

Journal

Neurology International, 15(3)

ISSN

2035-8385

Authors

Doher, Nicholas
Davoudi, Vahid
Magaki, Shino
[et al.](#)

Publication Date

2023-07-12



DOI

10.3390/neurolint15030054

Peer reviewed

Opinion

Illustrated Neuropathologic Diagnosis of Alzheimer's Disease

Nicholas Doher^{1,*}, Vahid Davoudi², Shino Magaki³, Ryan A. Townley^{4,5} , Mohammad Haeri^{2,5,*} 
and Harry V. Vinters^{3,6,7}¹ Department of Neurology, University of Florida, Gainesville, FL 32611, USA² Department of Pathology and Laboratory Medicine, University of Kansas Medical Center, Kansas City, KS 66160, USA³ Department of Pathology and Laboratory Medicine, David Geffen UCLA School of Medicine, Los Angeles, CA 90095, USA⁴ Department of Neurology, University of Kansas Medical Center, Kansas City, KS 66160, USA⁵ The University of Kansas Alzheimer's Disease Research Center, University of Kansas Medical Center, Fairway City, KS 66205, USA⁶ Department of Neurology, David Geffen UCLA School of Medicine, Los Angeles, CA 90095, USA⁷ Brain Research Institute, David Geffen UCLA School of Medicine, Los Angeles, CA 90095, USA

* Correspondence: ndoher@ufl.edu (N.D.); mhaeri@kumc.edu (M.H.)

Abstract: As of 2022, the prevalence of Alzheimer's disease (AD) among individuals aged 65 and older is estimated to be 6.2 million in the United States. This figure is predicted to grow to 13.8 million by 2060. An accurate assessment of neuropathologic changes represents a critical step in understanding the underlying mechanisms in AD. The current method for assessing postmortem Alzheimer's disease neuropathologic change follows version 11 of the National Alzheimer's Coordinating Center (NACC) coding guidebook. Ambiguity regarding steps in the ABC scoring method can lead to increased time or inaccuracy in staging AD. We present a concise overview of how this postmortem diagnosis is made and relate it to the evolving understanding of antemortem AD biomarkers.

Keywords: Alzheimer's disease; neurodegeneration; tauopathy; dementia; AD neuropathologic diagnosis



Citation: Doher, N.; Davoudi, V.; Magaki, S.; Townley, R.A.; Haeri, M.; Vinters, H.V. Illustrated Neuropathologic Diagnosis of Alzheimer's Disease. *Neurol. Int.* **2023**, *15*, 857–867. <https://doi.org/10.3390/neurolint15030054>

Academic Editor:
Benedetta Nacmias

Received: 14 March 2023
Revised: 6 June 2023
Accepted: 9 June 2023
Published: 12 July 2023



Copyright: © 2023 by the authors. Licensee MDPI, Basel, Switzerland. This article is an open access article distributed under the terms and conditions of the Creative Commons Attribution (CC BY) license (<https://creativecommons.org/licenses/by/4.0/>).

1. AD Antemortem Biomarkers

The advent of biomarkers has brought about a new era of improving the antemortem diagnostic accuracy of AD [1]. Biomarkers can be subdivided into biofluid-based laboratory tests such as amyloid- β 42 ($A\beta_{42}$) to amyloid- β 40 ($A\beta_{40}$) ratio ($A\beta_{42/40}$), total tau (T-tau), phosphorylated tau (P-tau), and neurofilament light (NfL) and diagnostic imaging, including positron emission tomography (PET) scans targeting glucose metabolism, amyloid- β , or tau deposition in the brain with unique ligands. Together with structural MRI, these biomarkers form the framework of the A/T/N system for antemortem AD diagnosis defined by the National Institute on Aging and Alzheimer's Association (NIA-AA), where "A" refers to amyloid, "T" refers to tau, and "N" refers to neurodegeneration [2].

The cerebrospinal fluid (CSF) concentration of amyloid- β decreases in patients with AD and correlates with the formation of neuritic plaques in the brain, making this test an effective biomarker for AD pathology [3,4]. Subsequent studies demonstrated that the ratio of $A\beta_{42}$ to $A\beta_{40}$ increases the specificity of predicting AD pathology antemortem [5]. $A\beta_{42}$ to $A\beta_{40}$ ratio ($A\beta_{42/40}$) is decreased in AD patients due to intraparenchymal accumulation [5]. PET scans targeting amyloids correlate with the typical progression of amyloid deposition in different brain regions found at autopsy [6–9]. In one study, amyloid PET data was used to assess 667 patients, and the study found a regional hierarchy of amyloid deposition that resembled previously defined neuropathologic findings [10]. It is important to note that roughly 30% of cognitively normal patients are amyloid-PET-positive, but it is

unclear if this cohort of patients represents preclinical AD or subjects at increased risk for AD [11].

CSF P-tau is relatively specific for AD pathology compared to other neurodegenerative diseases [12] and correlates well with NFT burden [4,13–15]. In general, the density of NFTs found at autopsy correlates better with cognitive status than the burden of amyloid- β plaques [16]. In research-oriented clinical practice, the increased levels of CSF T-tau are sensitive for neurodegenerative tauopathies [17], and it has been shown that phosphorylated tau markers such as P-tau181 and P-tau217 are particularly specific for AD pathologic process [18]. With regards to tau PET imaging, the topographic pattern has been shown to correlate with clinical AD progression [19–21] and more recently with postmortem Braak staging [22].

NfL is a non-specific marker of neuro-axonal damage and is elevated in the CSF of AD patients [23] as well as patients with dementia with Lewy bodies, Parkinson's disease dementia, frontotemporal dementia, vascular dementia, Creutzfeldt–Jakob disease, and amyotrophic lateral sclerosis [24–26]. High CSF levels of NfL have been shown to predict cognitive decline [27,28] and show a strong correlation with neuro-axonal damage and possibly cognition when measured in the plasma [29,30]. In a small study involving 26 patients, p-tau181 and NfL antemortem biomarkers correlated with postmortem-pathology-proven AD dementia [31]. Successful treatment of neurologic diseases such as multiple sclerosis [32] and spinal muscular atrophy [33] has resulted in reduction in NfL back to normal levels. This provides support for using NfL as a potential future marker of treatment response in neuro-axonal damage. Scans targeting F-18 fluorodeoxyglucose (FDG) to examine regional glucose metabolism can be combined with clinical assessment to improve diagnostic accuracy. Bloudek et al. compiled a meta-analysis including 119 studies and found FDG PET alone had a sensitivity of 92% (95% CI 84% to 96%) and specificity of 78% (95% CI 69% to 85%) in discriminating AD from non-AD demented controls [34]. Tripathi et al. found 93.4% concordance by combining clinical diagnosis with FDG PET results [35].

2. Diagnosis of Alzheimer's Disease Neuropathologic Change (ADNC)

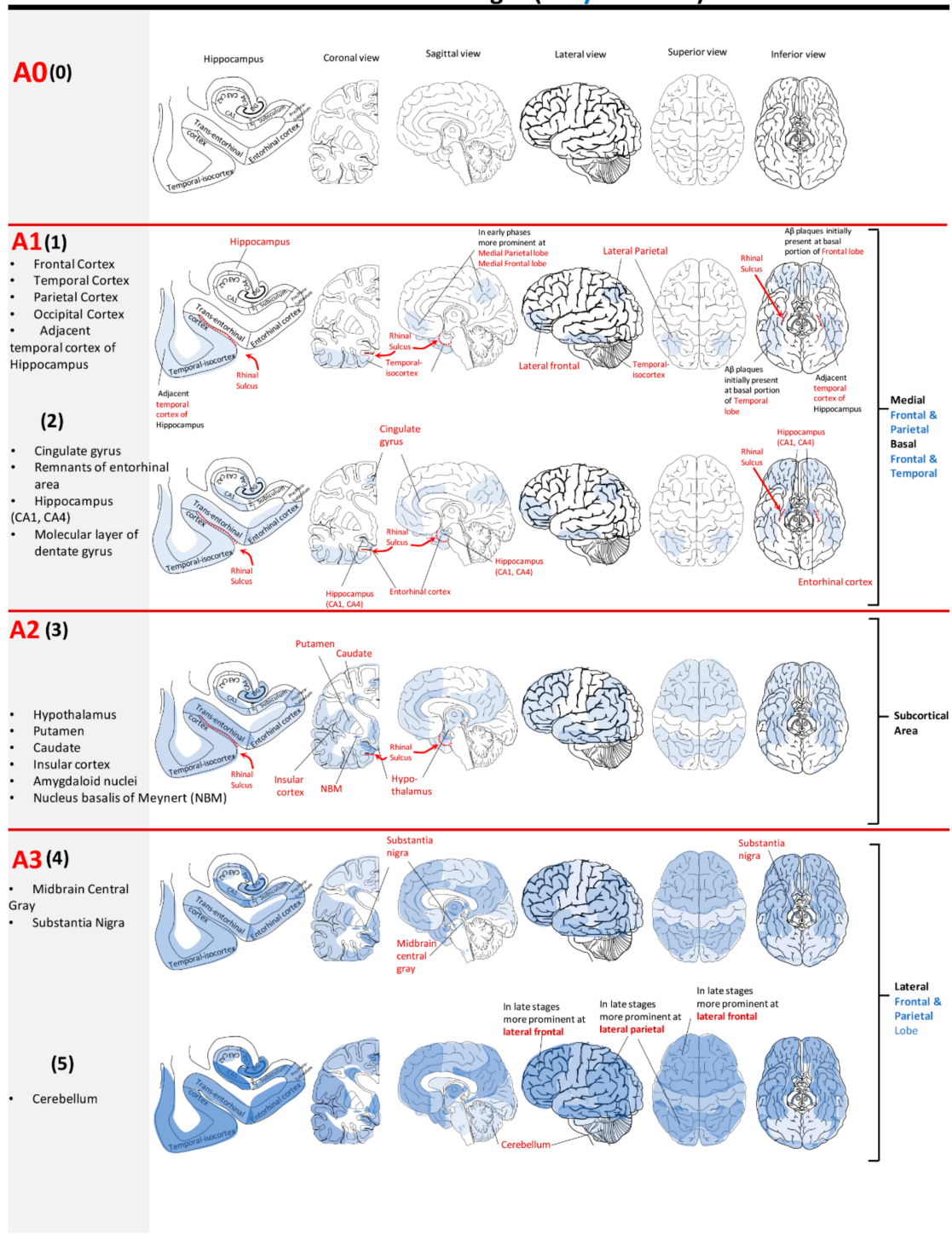
The hallmark neuropathologic changes seen in AD are neurofibrillary tangles (NFTs) composed of hyperphosphorylated tau protein aggregates and amyloid- β deposition, most specifically neuritic plaques (NP). Neuritic plaques have been described as a subset of senile plaques in which a central core of amyloid- β deposits is surrounded by a cluster of dystrophic neurites, frequently immunoreactive with phospho-tau antibodies [36,37].

Additional neuropathologic changes include cerebral amyloid angiopathy; neuronal and synaptic loss; granulovacuolar degeneration, which is usually confined to the hippocampus; and neuroinflammation [16]. The postmortem diagnosis of ADNC involves assessing amyloid and tau protein deposition that typically progresses in a predictable manner but differ in their chronology and topography. Tau deposition and progression show the strongest correlation with clinical disease stage [16]. In 2012, postmortem examinations were refined [36] to incorporate semi-quantitative measures of the pathologic hallmarks of AD. This framework utilizes a scoring system to inform the probability that ADNC explains a clinical diagnosis. An ABC scoring system uses four-point scales (0–3) where “A” correlates with “amyloid” or Thal phase, “B” correlates with tau or “Braak” stage, and “C” corresponds to neuritic plaque density in the neocortex based on the Consortium to Establish a Registry for Alzheimer's Disease (CERAD) score [38,39].

The A-score is derived from 5 Thal phases (Figure 1) [38] and staged from 0 to 3 depending on the distribution of APs [38]. It does not discriminate between amyloid plaque morphology or density. An A-score of “0” denotes an absence of amyloid in immunohistochemistry. Amyloid- β deposition begins in the neocortex (Thal phase 1), most commonly in the frontal lobe, and progresses posteriorly, involving association cortices in the temporal, parietal, and occipital lobes. Next, it progresses to the allocortex, including the entorhinal cortex, hippocampal region, and cingulate gyrus (Thal phase 2). Thal phases 1 and 2 are combined into stage A1. When amyloid- β is present in the striatum and the

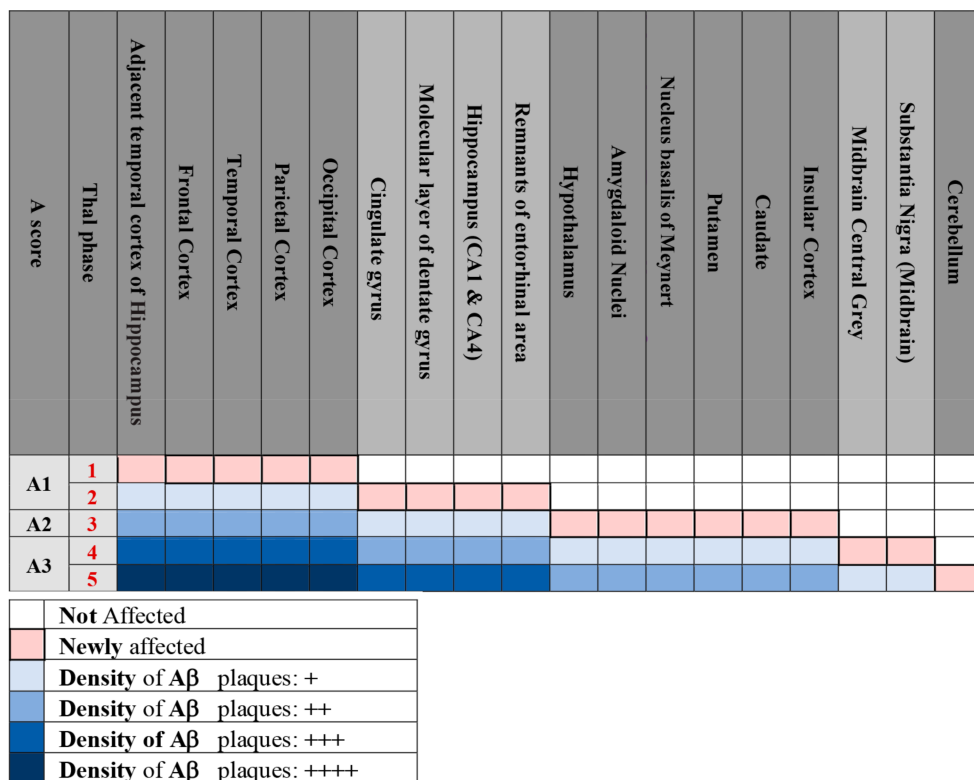
subcortical nuclei, such as the nucleus basalis of Meynert, it is stage “A2” (Thal phase 3). Finally, if amyloid-β is present in the midbrain, pons (Thal phase 4), or the cerebellum (Thal phase 5), the score is “A3”.

Thal stages (Amyloid beta)



(a)

Figure 1. Cont.

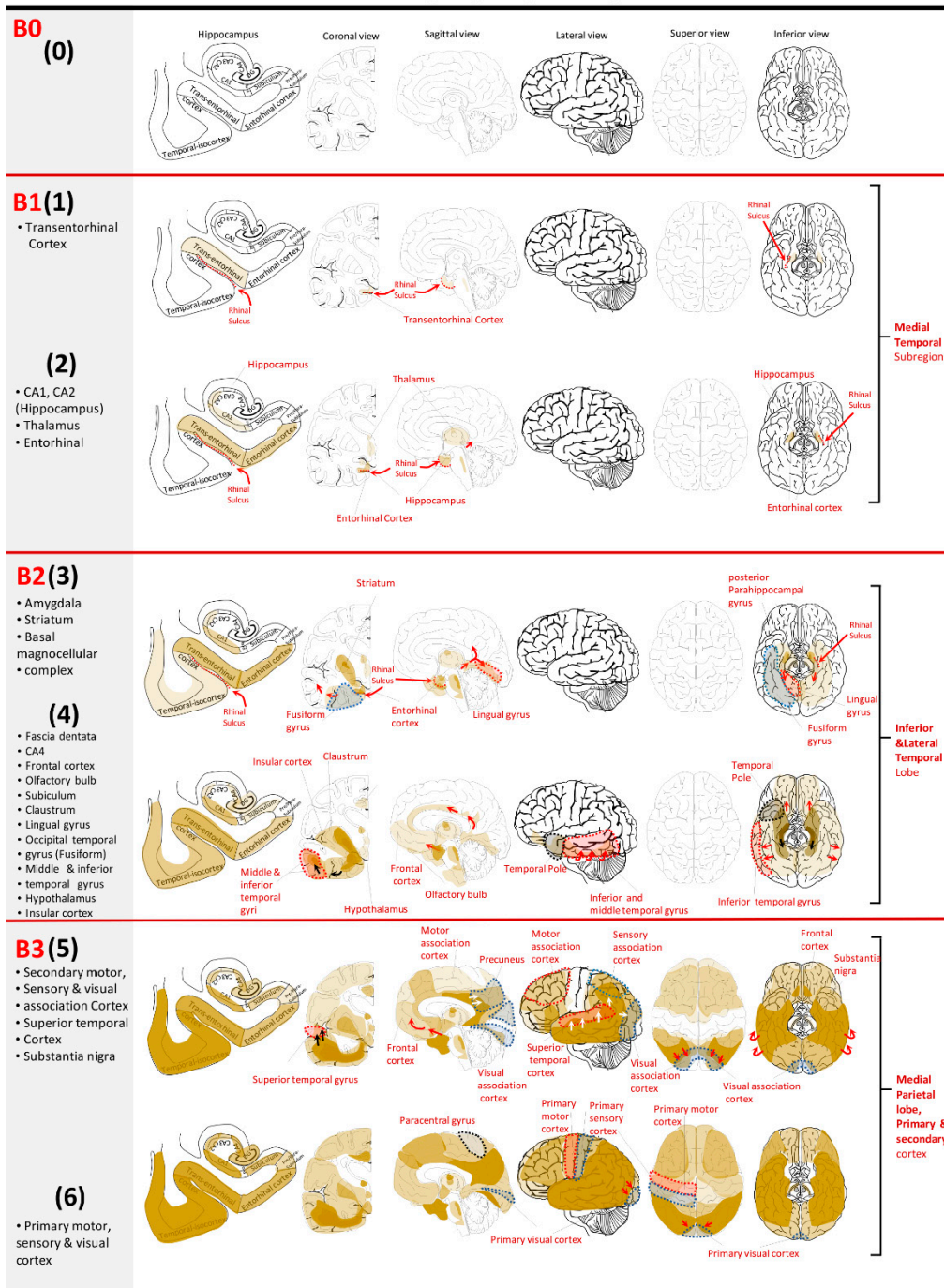


(b)

Figure 1. (a) Topographical map represents areas of Aβ accumulation (in blue) according to Thal phases and “A” score [38,40,41]. (b) Tabulated representation of the data. A1 (1). Aβ plaques begin in the frontal lobe and move posteriorly to affect parietal, temporal, and occipital lobes. They initially accumulate in the basal portion of the frontal and temporal lobes and temporal cortex adjacent to the hippocampus. In the early phases, Aβ plaques can be prominently observed in the medial frontal and medial parietal lobes. A1 (2). In the second phase, they involve cingulate gyrus. Medial temporal regions including entorhinal cortex and hippocampus (CA4 and CA1) are affected as well. A2 (3). Subcortical areas including hypothalamus, putamen, caudate, amygdaloid nuclei, and nucleus basalis of Meynert are affected in this stage. Aβ plaques expand further into the frontal, parietal, temporal, and occipital lobes and affect the insular cortex. A3 (4). Aβ plaques can be observed in the midbrain central gray, locus coeruleus, and substantia nigra. In this phase, the primary motor and sensory cortices are affected. A3 (5). The last phase is characterized by Aβ immunoreactivity in the cerebellum.

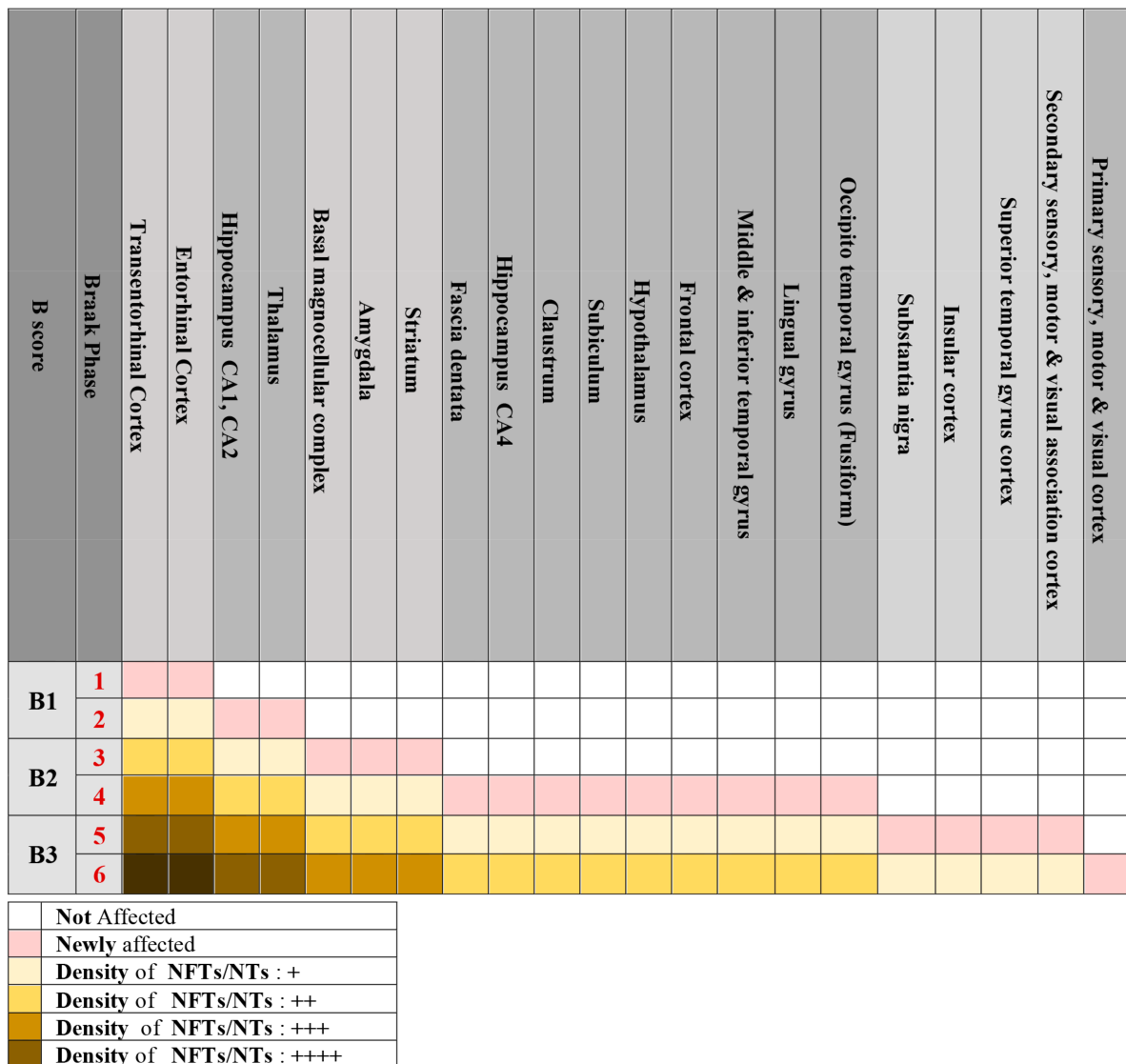
The B-score is derived from the Braak staging system (Figure 2) [42,43]. It is also scored on a 4-point scale of 0–3 and is based on a progression of abnormal tau protein in the form of NFTs, which are an integral part of AD pathology, and dystrophic neurites found in the periphery of NPs. As with the A-score, “0” denotes an absence of tau from immunohistochemical staining. Subsequent B-scores are based on Braak staging, beginning with the transentorhinal cortex (Stage I) and expanding to the entorhinal cortex and hippocampus (Stage II). Tau deposition subsequently involves the temporal neocortex, including occipito-temporal and lingual gyrus (Stage III), and more laterally expands to involve the middle temporal gyrus (Stage IV). Finally, tau aggregates spread to the remaining cortex (Stage V–VI), and the basal ganglia can also be involved in some cases. Accordingly, stage I–II, stage III–IV, and stage V–VI are scored as B1, B2, and B3, respectively [38].

Braak stages (Tau protein)



(a)

Figure 2. Cont.



(b)

Figure 2. (a) Topographical map represents areas of tau aggregation (in gold/brown). (b) Tabulated representation of the data. B1 (1). Initial phase of tau aggregation is largely confined to the transentorhinal cortex in the medial temporal area, although there may be minimal involvement of the entorhinal cortex. B1 (2). Lesions extend into the entorhinal cortex and CA1/CA2 of the hippocampus. B2 (3). Subsequently, tau accumulates in the basal magnocellular complex, amygdala, and striatum [42] (while not a constant finding) and spreads posteriorly through the posterior parahippocampal gyrus into lingual gyri and laterally from the medial temporal region to the occipito-temporal gyrus (fusiform gyrus). B2 (4). Tau propagates further anteriorly into the frontal lobe and laterally to the inferior and middle temporal cortex. Fascia dentata and CA4 region of the hippocampus may be affected in this phase. B3 (5). Tau aggregates extend into secondary cortical areas including motor, sensory, and visual association cortices. From the posterior cingulate gyrus, they spread posteriorly and affect the precuneus in the medial parietal lobe. Furthermore, tau encompasses other anatomical areas, including superior temporal cortex and pars compacta of substantia nigra. B3 (6). In the last phase, tau spreads into primary motor, sensory, and visual cortices [43].

The final component of the ABC scoring system, the C-score (Figure 3), is based on the NP density in the neocortex according to the CERAD protocol [39]. Very simply, the density of NPs is scored as C0, C1, C2, or C3, which denote absent, sparse, moderate, or

frequent NPs, respectively; templates from CERAD papers can be used as guides for this assessment [39]. It is important to note that diffuse plaques are not counted in this density assessment. This last component of the scoring system accounts for the importance of NP density as both a marker for AD neuropathology and an independent predictor of cognitive status antemortem [16].

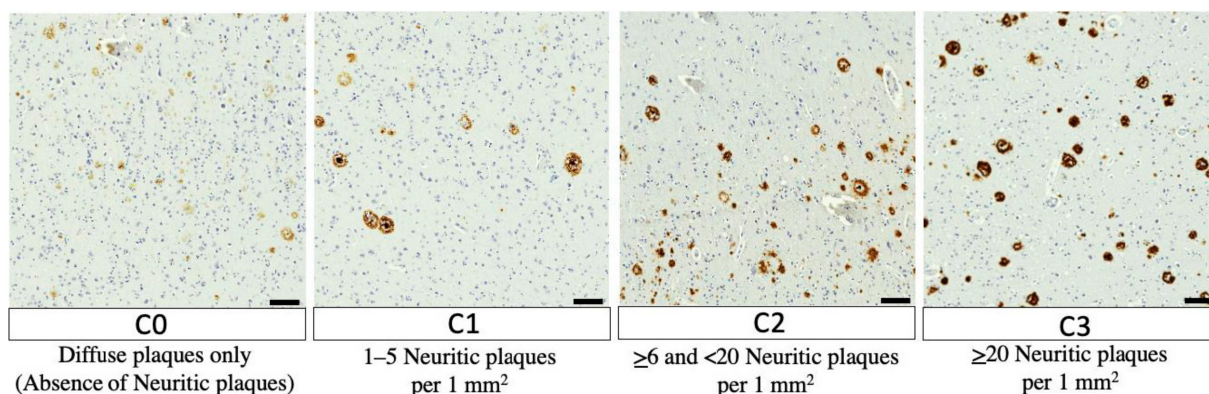


Figure 3. Updated CERAD scoring [38], Scale bars are 100 μm. Examples of senile plaque density for each CERAD score on immunohistochemistry using mouse anti-human β-amyloid (6F3D) antibody [44].

The final step is determining the likelihood that the neuropathologic findings explain the antemortem clinical syndrome based on the assigned ABC score as “not” (i.e., not AD), “low”, “intermediate”, or “high” according to Montine et al. [38] (Table 1). For example, the highest score, A3B3C3, corresponds to a “high” likelihood that the Alzheimer’s disease neuropathologic changes explain the clinical syndrome, whereas a score of A1B2C1 corresponds to a “low” likelihood.

Table 1. ABC Scoring (extracted from Montine et al.) [38].

AD Pathology		B; NFT Braak Stage ^a		
A; β-Amyloid ^b Thal Phase > Score	C; CERAD ^c Plaque Density	0 or 1	2	3
0	0	Not ^d	Not ^d	Not ^d
1	0 or 1	Low	Low	Low ^e
	2 or 3 ^f	Low	Intermediate	Intermediate ^e
2	Any C	Low ^g	Intermediate	Intermediate ^e
3	0 or 1	Low ^g	Intermediate	Intermediate ^e
	2 or 3	Low ^g	Intermediate	High

ABC scoring combines different possibilities of AD neuropathologic changes and generates a qualitative score including “Not” (i.e., not AD), “Low”, “Intermediate”, and “High”. Intermediate or High better justify the AD diagnosis for clinical dementia [38].^a NFT Braak stage [42,43],^b Thal beta-amyloid plaque phase/score [40], and^c CERAD senile plaque score [39] are essential for ABC scoring.^d Presence of NFTs in medial temporal regions without Aβ or senile plaques can be due to aging. It can also be seen in subjects with mild cognitive impairment or in those whose cognitive impairment is due to other causes rather than AD [45].^e In cases with extensive NFTs and low level of amyloid plaques, other tauopathies should be considered.^f High density of senile plaques with a low Thal phase warrants reassessment of senile/diffuse plaques, considering the contribution of other diseases to cognitive impairment or dementia.^g In the setting of high Aβ burden with low Braak stage, co-morbidities such as Lewy body disease, vascular brain injury, or hippocampal sclerosis can be considered. Additional sections should be studied to evaluate other non-AD pathologies [38].

3. Alzheimer’s Dementia Clinical Subtypes

Historically, AD has been characterized by progressive impairment in episodic memory, executive function, language, and visuospatial function, with the most prominent deficits in memory [25,46,47]. Thanks to new PET imaging techniques, it is possible to

map the spread of tau in different brain regions of living subjects. In vivo observations in these imaging studies have been shown to have significant compatibility with classic Braak staging [48–52]. Since the advent of CSF biomarkers, molecular neuroimaging, and neuropsychological evaluations, four distinct subtypes have emerged: limbic-predominant, medial temporal lobe (MTL)-sparing, posterior, and lateral temporal [53]. These subtypes are based on in vivo tau deposition and have a strong correlation between corticolimbic network involvement and expected clinical presentation and progression. The limbic subtype most closely resembles the classical amnesic predominant presentation and progression of AD. On average, patients with the limbic subtype have worse delayed-recall memory but initially perform better across other cognitive domains compared to other subtypes. Tau progression in the limbic subtype starts in the entorhinal cortex and follows the typical pattern noted by the Braak staging scheme. This group is also more likely to include APOE4 carriers and have an older age of onset. Patients with the MTL-sparing subtype tend to be younger at onset, with an overall higher tau burden in the frontoparietal networks and more prominent deficits in executive function and working memory [53]. New reports demonstrate evidence of neuropathologic findings seen in the MTL-sparing subtype [54] showing a possible different pathway of pTAU pathology that first involves parietal cortex, followed by limbic structures. The posterior subtype shows prominent deficits in visuospatial functions and corresponds with the clinical phenotype of posterior cortical atrophy [47]. Finally, the lateral temporal subtype, particularly when lateralized to the dominant hemisphere, is characterized by more prominent language involvement and corresponds with the clinical phenotype of logopenic variant primary progressive aphasia. Taken together, these subtypes explain much of the heterogeneity seen among AD patients and have significant implications for patient counseling on prognosis, symptom progression, and targeted therapy in the future.

4. Discussion

Alzheimer's disease continues to be the sixth-leading cause of death in the United States, with total payments to health care, long-term care, and hospice care estimated to be \$355 billion (AD facts and figures 2021) [55]. Therapeutic research efforts have focused on amyloid- β protein and tau aggregates, emphasizing the importance of an accurate postmortem neuropathologic diagnosis of Alzheimer's disease to support antemortem biomarkers and clinical diagnoses [2,56]. The ability to establish a confident antemortem diagnosis has significant implications for future research and allows families to make informed decisions for the future. Furthermore, the addition of Alzheimer's dementia clinical phenotypes has put a spotlight on specific patterns of pathological change. It is hoped that this summary of the ABC scoring system will be a useful reference for AD scientists, clinicians, neurologists, neuropathologists, and general pathologists and provide a better understanding of the diagnosis and staging of Alzheimer's disease with efficiency and accuracy. Additionally, this work is aimed at assisting scientists working on preclinical models of AD to ensure that their work can be translated to the clinic.

Author Contributions: N.D. and V.D. wrote the manuscript with M.H.'s assistance and feedback. S.M. gave feedback on the neuropathologic diagnosis segment and edited the entire manuscript. R.A.T. commented on clinical correlation. M.H. supervised the manuscript and assisted with illustration preparation and writing. H.V.V. edited the entire manuscript for its accuracy and clarity. All authors have read and agreed to the published version of the manuscript.

Funding: This work is supported by a startup fund provided by the University of Kansas to Mohammad Haeri and the P30 grant from the NIH/NIA to the University of Kansas Alzheimer Disease Research Center (P30 AG072973).

Institutional Review Board Statement: Not applicable.

Informed Consent Statement: Not applicable.

Data Availability Statement: No new data were created or analyzed in this study. Data sharing is not applicable to this article.

Conflicts of Interest: The authors declare no conflict of interest.

References

- Gessi, S.; Poloni, T.E.; Negro, G.; Varani, K.; Pasquini, S.; Vincenzi, F.; Borea, P.A.; Merighi, S. A(2A) Adenosine Receptor as a Potential Biomarker and a Possible Therapeutic Target in Alzheimer's Disease. *Cells* **2021**, *10*, 2344. [[CrossRef](#)] [[PubMed](#)]
- Jack, C.R., Jr.; Bennett, D.A.; Blennow, K.; Carrillo, M.C.; Dunn, B.; Haeberlein, S.B.; Holtzman, D.M.; Jagust, W.; Jessen, F.; Karlawish, J.; et al. NIA-AA Research Framework: Toward a biological definition of Alzheimer's disease. *Alzheimers Dement.* **2018**, *14*, 535–562. [[CrossRef](#)]
- Masters, C.L.; Selkoe, D.J. Biochemistry of amyloid β -protein and amyloid deposits in Alzheimer disease. *Cold Spring Harb. Perspect. Med.* **2012**, *2*, a006262. [[CrossRef](#)]
- Tapiola, T.; Alafuzoff, I.; Herukka, S.K.; Parkkinen, L.; Hartikainen, P.; Soininen, H.; Pirttilä, T. Cerebrospinal fluid β -amyloid 42 and tau proteins as biomarkers of Alzheimer-type pathologic changes in the brain. *Arch. Neurol.* **2009**, *66*, 382–389. [[CrossRef](#)]
- Hansson, O.; Lehmann, S.; Otto, M.; Zetterberg, H.; Lewczuk, P. Advantages and disadvantages of the use of the CSF Amyloid β ($A\beta$) 42/40 ratio in the diagnosis of Alzheimer's Disease. *Alzheimer's Res. Ther.* **2019**, *11*, 34. [[CrossRef](#)]
- Clark, C.M.; Schneider, J.A.; Bedell, B.J.; Beach, T.G.; Bilker, W.B.; Mintun, M.A.; Pontecorvo, M.J.; Hefti, F.; Carpenter, A.P.; Flitter, M.L. Use of florbetapir-PET for imaging β -amyloid pathology. *Jama* **2011**, *305*, 275–283. [[CrossRef](#)] [[PubMed](#)]
- Clark, C.M.; Pontecorvo, M.J.; Beach, T.G.; Bedell, B.J.; Coleman, R.E.; Doraiswamy, P.M.; Fleisher, A.S.; Reiman, E.M.; Sabbagh, M.N.; Sadowsky, C.H. Cerebral PET with florbetapir compared with neuropathology at autopsy for detection of neuritic amyloid- β plaques: A prospective cohort study. *Lancet Neurol.* **2012**, *11*, 669–678. [[CrossRef](#)]
- Wolk, D.A.; Grachev, I.D.; Buckley, C.; Kazi, H.; Grady, M.S.; Trojanowski, J.Q.; Hamilton, R.H.; Sherwin, P.; McLain, R.; Arnold, S.E. Association between in vivo fluorine 18-labeled flutemetamol amyloid positron emission tomography imaging and in vivo cerebral cortical histopathology. *Arch. Neurol.* **2011**, *68*, 1398–1403. [[CrossRef](#)]
- Ikonomovic, M.D.; Klunk, W.E.; Abrahamson, E.E.; Mathis, C.A.; Price, J.C.; Tsopelas, N.D.; Lopresti, B.J.; Ziolkko, S.; Bi, W.; Paljug, W.R. Post-mortem correlates of in vivo PiB-PET amyloid imaging in a typical case of Alzheimer's disease. *Brain* **2008**, *131*, 1630–1645. [[CrossRef](#)] [[PubMed](#)]
- Grothe, M.J.; Barthel, H.; Sepulcre, J.; Dyrba, M.; Sabri, O.; Teipel, S.J.; Alzheimer's Disease Neuroimaging Initiative. In vivo staging of regional amyloid deposition. *Neurology* **2017**, *89*, 2031–2038. [[CrossRef](#)]
- Jack, C.R.; Barrio, J.R.; Kepe, V. Cerebral amyloid PET imaging in Alzheimer's disease. *Acta Neuropathol.* **2013**, *126*, 643–657. [[CrossRef](#)]
- Itoh, N.; Arai, H.; Urakami, K.; Ishiguro, K.; Ohno, H.; Hampel, H.; Buerger, K.; Wiltfang, J.; Otto, M.; Kretschmar, H.; et al. Large-scale, multicenter study of cerebrospinal fluid tau protein phosphorylated at serine 199 for the antemortem diagnosis of Alzheimer's disease. *Ann. Neurol.* **2001**, *50*, 150–156. [[CrossRef](#)] [[PubMed](#)]
- Clark, C.M.; Xie, S.; Chittams, J.; Ewbank, D.; Peskind, E.; Galasko, D.; Morris, J.C.; McKeel, D.W.; Farlow, M.; Weitlauf, S.L. Cerebrospinal fluid tau and β -amyloid: How well do these biomarkers reflect autopsy-confirmed dementia diagnoses? *Arch. Neurol.* **2003**, *60*, 1696–1702. [[CrossRef](#)]
- Buerger, K.; Ewers, M.; Pirttilä, T.; Zinkowski, R.; Alafuzoff, I.; Teipel, S.J.; DeBernardis, J.; Kerkman, D.; McCulloch, C.; Soininen, H. CSF phosphorylated tau protein correlates with neocortical neurofibrillary pathology in Alzheimer's disease. *Brain* **2006**, *129*, 3035–3041. [[CrossRef](#)] [[PubMed](#)]
- De Souza, L.C.; Chupin, M.; Lamari, F.; Jardel, C.; Leclercq, D.; Colliot, O.; Lehéricy, S.; Dubois, B.; Sarazin, M. CSF tau markers are correlated with hippocampal volume in Alzheimer's disease. *Neurobiol. Aging* **2012**, *33*, 1253–1257. [[CrossRef](#)] [[PubMed](#)]
- Nelson, P.T.; Alafuzoff, I.; Bigio, E.H.; Bouras, C.; Braak, H.; Cairns, N.J.; Castellani, R.J.; Crain, B.J.; Davies, P.; Tredici, K.D. Correlation of Alzheimer disease neuropathologic changes with cognitive status: A review of the literature. *J. Neuropathol. Exp. Neurol.* **2012**, *71*, 362–381. [[CrossRef](#)]
- Blennow, K.; Wallin, A.; Ågren, H.; Spenger, C.; Siegfried, J.; Vanmechelen, E. Tau protein in cerebrospinal fluid. *Mol. Chem. Neuropathol.* **1995**, *26*, 231–245. [[CrossRef](#)]
- Thijssen, E.H.; La Joie, R.; Strom, A.; Fonseca, C.; Iaccarino, L.; Wolf, A.; Spina, S.; Allen, I.E.; Cobigo, Y.; Heuer, H.; et al. Plasma phosphorylated tau 217 and phosphorylated tau 181 as biomarkers in Alzheimer's disease and frontotemporal lobar degeneration: A retrospective diagnostic performance study. *Lancet Neurol.* **2021**, *20*, 739–752. [[CrossRef](#)]
- Brier, M.R.; Gordon, B.; Friedrichsen, K.; McCarthy, J.; Stern, A.; Christensen, J.; Owen, C.; Aldea, P.; Su, Y.; Hassenstab, J. Tau and $A\beta$ imaging, CSF measures, and cognition in Alzheimer's disease. *Sci. Transl. Med.* **2016**, *8*, 338ra66. [[CrossRef](#)]
- Therriault, J.; Vermeiren, M.; Servaes, S.; Tissot, C.; Ashton, N.J.; Benedet, A.L.; Karikari, T.K.; Lantero-Rodriguez, J.; Brum, W.S.; Lussier, F.Z.; et al. Association of Phosphorylated Tau Biomarkers With Amyloid Positron Emission Tomography vs. Tau Positron Emission Tomography. *JAMA Neurol.* **2023**, *80*, 188–199. [[CrossRef](#)] [[PubMed](#)]
- Ossenkoppele, R.; Pichet Binette, A.; Groot, C.; Smith, R.; Strandberg, O.; Palmqvist, S.; Stomrud, E.; Tideman, P.; Ohlsson, T.; Jogi, J.; et al. Amyloid and tau PET-positive cognitively unimpaired individuals are at high risk for future cognitive decline. *Nat. Med.* **2022**, *28*, 2381–2387. [[CrossRef](#)] [[PubMed](#)]

22. Fleisher, A.S.; Pontecorvo, M.J.; Devous, M.D.; Lu, M.; Arora, A.K.; Truocchio, S.P.; Aldea, P.; Flitter, M.; Locascio, T.; Devine, M. Positron emission tomography imaging with [18F] flortaucipir and postmortem assessment of Alzheimer disease neuropathologic changes. *JAMA Neurol.* **2020**, *77*, 829–839. [[CrossRef](#)] [[PubMed](#)]
23. Olsson, B.; Lautner, R.; Andreasson, U.; Öhrfelt, A.; Portelius, E.; Bjerke, M.; Hölttä, M.; Rosén, C.; Olsson, C.; Strobel, G. CSF and blood biomarkers for the diagnosis of Alzheimer's disease: A systematic review and meta-analysis. *Lancet Neurol.* **2016**, *15*, 673–684. [[CrossRef](#)] [[PubMed](#)]
24. Skillbäck, T.; Farahmand, B.; Bartlett, J.W.; Rosén, C.; Mattsson, N.; Nägga, K.; Kilander, L.; Religa, D.; Wimo, A.; Winblad, B. CSF neurofilament light differs in neurodegenerative diseases and predicts severity and survival. *Neurology* **2014**, *83*, 1945–1953. [[CrossRef](#)] [[PubMed](#)]
25. Abu-Rumeileh, S.; Capellari, S.; Stanzani-Maserati, M.; Polischi, B.; Martinelli, P.; Caroppo, P.; Ladogana, A.; Parchi, P. The CSF neurofilament light signature in rapidly progressive neurodegenerative dementias. *Alzheimer's Res. Ther.* **2018**, *10*, 3. [[CrossRef](#)]
26. Wang, S.-Y.; Chen, W.; Xu, W.; Li, J.-Q.; Hou, X.-H.; Ou, Y.-N.; Yu, J.-T.; Tan, L. Neurofilament light chain in cerebrospinal fluid and blood as a biomarker for neurodegenerative diseases: A systematic review and meta-analysis. *J. Alzheimer's Dis.* **2019**, *72*, 1353–1361. [[CrossRef](#)]
27. Zetterberg, H.; Skillbäck, T.; Mattsson, N.; Trojanowski, J.Q.; Portelius, E.; Shaw, L.M.; Weiner, M.W.; Blennow, K.; Initiative, A.s.D.N. Association of cerebrospinal fluid neurofilament light concentration with Alzheimer disease progression. *JAMA Neurol.* **2016**, *73*, 60–67. [[CrossRef](#)]
28. Mielke, M.M.; Syrjanen, J.A.; Blennow, K.; Zetterberg, H.; Vemuri, P.; Skoog, I.; Machulda, M.M.; Kremers, W.K.; Knopman, D.S.; Jack, C. Plasma and CSF neurofilament light: Relation to longitudinal neuroimaging and cognitive measures. *Neurology* **2019**, *93*, e252–e260. [[CrossRef](#)]
29. He, L.; Morley, J.E.; Aggarwal, G.; Nguyen, A.D.; Vellas, B.; de Souto Barreto, P. Plasma neurofilament light chain is associated with cognitive decline in non-dementia older adults. *Sci. Rep.* **2021**, *11*, 13394. [[CrossRef](#)] [[PubMed](#)]
30. Lin, Y.-S.; Lee, W.-J.; Wang, S.-J.; Fuh, J.-L. Levels of plasma neurofilament light chain and cognitive function in patients with Alzheimer or Parkinson disease. *Sci. Rep.* **2018**, *8*, 17368. [[CrossRef](#)]
31. Grothe, M.J.; Moscoso, A.; Ashton, N.J.; Karikari, T.K.; Lantero-Rodriguez, J.; Snellman, A.; Zetterberg, H.; Blennow, K.; Schöll, M.; Initiative, A.s.D.N. Associations of fully automated CSF and novel plasma biomarkers with Alzheimer disease neuropathology at autopsy. *Neurology* **2021**, *97*, e1229–e1242. [[CrossRef](#)]
32. Gunnarsson, M.; Malmeström, C.; Axelsson, M.; Sundström, P.; Dahle, C.; Vrethem, M.; Olsson, T.; Piehl, F.; Norgren, N.; Rosengren, L. Axonal damage in relapsing multiple sclerosis is markedly reduced by natalizumab. *Ann. Neurol.* **2011**, *69*, 83–89. [[CrossRef](#)]
33. Olsson, B.; Alberg, L.; Cullen, N.C.; Michael, E.; Wahlgren, L.; Kroksmark, A.-K.; Rostasy, K.; Blennow, K.; Zetterberg, H.; Tulinius, M. NFL is a marker of treatment response in children with SMA treated with nusinersen. *J. Neurol.* **2019**, *266*, 2129–2136. [[CrossRef](#)]
34. Bloudek, L.M.; Spackman, D.E.; Blankenburg, M.; Sullivan, S.D. Review and meta-analysis of biomarkers and diagnostic imaging in Alzheimer's disease. *J. Alzheimer's Dis.* **2011**, *26*, 627–645. [[CrossRef](#)]
35. Tripathi, M.; Tripathi, M.; Damle, N.; Kushwaha, S.; Jaimini, A.; D'Souza, M.M.; Sharma, R.; Saw, S.; Mondal, A. Differential diagnosis of neurodegenerative dementias using metabolic phenotypes on F-18 FDG PET/CT. *Neuroradiol. J.* **2014**, *27*, 13–21. [[CrossRef](#)] [[PubMed](#)]
36. Hyman, B.T.; Phelps, C.H.; Beach, T.G.; Bigio, E.H.; Cairns, N.J.; Carrillo, M.C.; Dickson, D.W.; Duyckaerts, C.; Frosch, M.P.; Masliah, E. National Institute on Aging–Alzheimer's Association guidelines for the neuropathologic assessment of Alzheimer's disease. *Alzheimer's Dement.* **2012**, *8*, 1–13. [[CrossRef](#)] [[PubMed](#)]
37. Thal, D.R.; Rüb, U.; Schultz, C.; Sassin, I.; Ghebremedhin, E.; Del Tredici, K.; Braak, E.; Braak, H. Sequence of A β -protein deposition in the human medial temporal lobe. *J. Neuropathol. Exp. Neurol.* **2000**, *59*, 733–748. [[CrossRef](#)] [[PubMed](#)]
38. Montine, T.J.; Phelps, C.H.; Beach, T.G.; Bigio, E.H.; Cairns, N.J.; Dickson, D.W.; Duyckaerts, C.; Frosch, M.P.; Masliah, E.; Mirra, S.S. National Institute on Aging–Alzheimer's Association guidelines for the neuropathologic assessment of Alzheimer's disease: A practical approach. *Acta Neuropathol.* **2012**, *123*, 1–11. [[CrossRef](#)]
39. Mirra, S.S.; Heyman, A.; McKeel, D.; Sumi, S.; Crain, B.J.; Brownlee, L.; Vogel, F.; Hughes, J.; Van Belle, G.; Berg, L. The Consortium to Establish a Registry for Alzheimer's Disease (CERAD): Part II. Standardization of the neuropathologic assessment of Alzheimer's disease. *Neurology* **1991**, *41*, 479. [[CrossRef](#)]
40. Thal, D.R.; Rüb, U.; Orantes, M.; Braak, H. Phases of A β -deposition in the human brain and its relevance for the development of AD. *Neurology* **2002**, *58*, 1791–1800. [[CrossRef](#)]
41. Alafuzoff, I.; Thal, D.R.; Arzberger, T.; Bogdanovic, N.; Al-Sarraj, S.; Bodi, I.; Boluda, S.; Bugiani, O.; Duyckaerts, C.; Gelpi, E. Assessment of β -amyloid deposits in human brain: A study of the BrainNet Europe Consortium. *Acta Neuropathol.* **2009**, *117*, 309–320. [[CrossRef](#)]
42. Braak, H.; Braak, E. Neuropathological stageing of Alzheimer-related changes. *Acta Neuropathol.* **1991**, *82*, 239–259. [[CrossRef](#)]
43. Braak, H.; Alafuzoff, I.; Arzberger, T.; Kretschmar, H.; Del Tredici, K. Staging of Alzheimer disease-associated neurofibrillary pathology using paraffin sections and immunocytochemistry. *Acta Neuropathol.* **2006**, *112*, 389–404. [[CrossRef](#)] [[PubMed](#)]

44. Akiyama, H.; Mori, H.; Saido, T.; Kondo, H.; Ikeda, K.; McGeer, P.L. Occurrence of the diffuse amyloid beta-protein (A β) deposits with numerous A β -containing glial cells in the cerebral cortex of patients with Alzheimer's disease. *Glia* **1999**, *25*, 324–331. [[CrossRef](#)]
45. Nelson, P.T.; Abner, E.L.; Schmitt, F.A.; Kryscio, R.J.; Jicha, G.A.; Santacruz, K.; Smith, C.D.; Patel, E.; Markesbery, W.R. Brains with medial temporal lobe neurofibrillary tangles but no neuritic amyloid plaques are a diagnostic dilemma but may have pathogenetic aspects distinct from Alzheimer disease. *J. Neuropathol. Exp. Neurol.* **2009**, *68*, 774–784. [[CrossRef](#)] [[PubMed](#)]
46. Dubois, B.; Feldman, H.H.; Jacova, C.; Hampel, H.; Molinuevo, J.L.; Blennow, K.; DeKosky, S.T.; Gauthier, S.; Selkoe, D.; Bateman, R.; et al. Advancing research diagnostic criteria for Alzheimer's disease: The IWG-2 criteria. *Lancet Neurol.* **2014**, *13*, 614–629, Erratum in *Lancet Neurol.* **2014**, *13*, 757.
47. Townley, R.A.; Graff-Radford, J.; Mantyh, W.G.; Botha, H.; Polsinelli, A.J.; Przybelski, S.A.; Machulda, M.M.; Makhoul, A.T.; Senjem, M.L.; Murray, M.E.; et al. Progressive dysexecutive syndrome due to Alzheimer's disease: A description of 55 cases and comparison to other phenotypes. *Brain Commun.* **2020**, *2*, fcaa068. [[CrossRef](#)] [[PubMed](#)]
48. Schöll, M.; Lockhart, S.N.; Schonhaut, D.R.; O'Neil, J.P.; Janabi, M.; Ossenkoppele, R.; Baker, S.L.; Vogel, J.W.; Faria, J.; Schwimmer, H.D. PET imaging of tau deposition in the aging human brain. *Neuron* **2016**, *89*, 971–982. [[CrossRef](#)]
49. Cho, H.; Choi, J.Y.; Hwang, M.S.; Kim, Y.J.; Lee, H.M.; Lee, H.S.; Lee, J.H.; Ryu, Y.H.; Lee, M.S.; Lyoo, C.H. In vivo cortical spreading pattern of tau and amyloid in the Alzheimer disease spectrum. *Ann. Neurol.* **2016**, *80*, 247–258. [[CrossRef](#)]
50. Schwarz, A.J.; Yu, P.; Miller, B.B.; Shcherbinin, S.; Dickson, J.; Navitsky, M.; Joshi, A.D.; Devous, M.D., Sr.; Mintun, M.S. Regional profiles of the candidate tau PET ligand 18 F-AV-1451 recapitulate key features of Braak histopathological stages. *Brain* **2016**, *139*, 1539–1550. [[CrossRef](#)]
51. Johnson, K.A.; Schultz, A.; Betensky, R.A.; Becker, J.A.; Sepulcre, J.; Rentz, D.; Mormino, E.; Chhatwal, J.; Amariglio, R.; Papp, K. Tau positron emission tomographic imaging in aging and early Alzheimer disease. *Ann. Neurol.* **2016**, *79*, 110–119. [[CrossRef](#)]
52. Marquie, M.; Normandin, M.D.; Vanderburg, C.R.; Costantino, I.M.; Bien, E.A.; Rycyna, L.G.; Klunk, W.E.; Mathis, C.A.; Ikonovic, M.D.; Debnath, M.L. Validating novel tau positron emission tomography tracer [F-18]-AV-1451 (T807) on postmortem brain tissue. *Ann. Neurol.* **2015**, *78*, 787–800. [[CrossRef](#)]
53. Vogel, J.W.; Young, A.L.; Oxtoby, N.P.; Smith, R.; Ossenkoppele, R.; Strandberg, O.T.; La Joie, R.; Aksman, L.M.; Grothe, M.J.; Iturria-Medina, Y. Four distinct trajectories of tau deposition identified in Alzheimer's disease. *Nat. Med.* **2021**, *27*, 871–881. [[CrossRef](#)]
54. Ferreira, D.; Mohanty, R.; Murray, M.E.; Nordberg, A.; Kantarci, K.; Westman, E. The hippocampal sparing subtype of Alzheimer's disease assessed in neuropathology and in vivo tau positron emission tomography: A systematic review. *Acta Neuropathol. Commun.* **2022**, *10*, 166. [[CrossRef](#)] [[PubMed](#)]
55. Monica Moore, M.; Díaz-Santos, M.; Vossel, K. 2021 Alzheimer's disease facts and figures. *Alzheimers Dement.* **2021**, *17*, 327–406. [[CrossRef](#)]
56. Brodaty, H.; Seeher, K.; Gibson, L. Dementia time to death: A systematic literature review on survival time and years of life lost in people with dementia. *Int. Psychogeriatr.* **2012**, *24*, 1034–1045. [[CrossRef](#)] [[PubMed](#)]

Disclaimer/Publisher's Note: The statements, opinions and data contained in all publications are solely those of the individual author(s) and contributor(s) and not of MDPI and/or the editor(s). MDPI and/or the editor(s) disclaim responsibility for any injury to people or property resulting from any ideas, methods, instructions or products referred to in the content.